Research Paper

A facile synthesis method and spectral characterization of silicon dioxide and magnetite nanoparticles

R. El-Shiekh[a], Mostafa Y. Nassar[b], W. H. El-Shiwiny[a], Hamed I. El-Salhy[a]

[a]Chemistry Department, Faculty of Science, Zagazig University, Zagazig 44519, Egypt
[b]Chemistry Department, Faculty of Science, Benha University, Benha 13815, Egypt

Abstract: Nanomaterials have attracted the tremendous interest of a vast number of researchers due to their unique characteristics. Metallic nanoparticles, especially magnetite nanoparticles (M) have thermal, mechanical, optical, electrical, and magnetic properties that differ from those of the bulk material enabling these nanoparticles to be applied in a huge number of application fields such as; industrial, medical, engineering, and scientific research. Also, ceramic nanoparticles such as silicon dioxide nanoparticles(S) due to their high porosity, high surface-to-volume ratio, and biocompatibility, they are used broadly in many applications increasingly. The preparation of these nanoparticles has become a highly demand. Therefore, the hydrothermal method to synthesize magnetite nanoparticles exhibited a good result in producing a cubic crystal with a low crystal size of 4 nm in a facile procedure. Silica nanoparticles were fabricated via a simple preparation method, the sol-gel method using a nontoxic precursor with a crystal size of 37 nm. The characterization of the as-prepared nanoparticles was attempted using x-ray diffraction (XRD), infra-red (IR) spectra, energy-dispersive x-ray spectroscopy (EDS), transmission electron microscope (TEM), and scanning electron microscope (SEM), and the results showed that the fabricated nanoparticles have a crystal phase with identified particles and morphological shapes.

--- -----

Date of Submission: 09-08-2022   Date of acceptance: 14-09-2022

-- ---------

I. INTRODUCTION

Nanoparticles are the cornerstone of nanotechnology which is the ability to work at the atomic or the molecular scale[1]. The dimensions of nanoparticles are among the dimensions of ions and those of bulk materials, and their ranges are 1-1000 nm[2, 3]. They have the important potential for applications in the different fields such as materials sciences, mechanics, physics, chemistry, biology, and medicine. Synthesis and characterization of nanostructured materials is a subject of great interest both in basic research and in the technological applications [4].

Ceramic nanoparticles are inorganic substances with a porous property, and they are carbonates, oxides, and phosphates of metalloids and metals such as silicon. These nanoparticles (NPs) can be synthesized via many available and low-cost simple methods, and their size, shape, and particle distribution can be controlled, and they have been applied in a vast number of the applications[5-7]. Silica nanostructures have been employed widely in a large number of applications such as water treatment, biomedical fields, and engineering applications due to their high porosity, nontoxicity, high surface area and pore volume, the availability of hydroxy functional groups on their surface, simple preparation methods, easy control of particle size and morphology, and easy control of physicochemical properties[8]. Magnetite nanoparticles, on the other hand, are one of the important and widely studied nanomaterials in various application fields, and they are ideal oxide support due to their easy fabrication methods, their surface activity for adsorption of ligands, low toxicity, magnetic properties, and biocompatibility[9]. Magnetite nanoparticles has a unique structure, they contains a divalent and trivalent in the same molecule with the stoichiometric ratio of Fe^{2+}: $2Fe^{3+}$ in a face-centered cubic crystallographic structure, where the Fe^{2+} ions align their spins parallel to Fe^{3+} ions in adjacent octahedral sites leading to a net magnetization. Magnetite has high biocompatibility, therefor they are broadly utilized in the biomedical field; in magnetic resonance imaging (MRI)

as contrast agents, magnetic hyperthermia, gene delivery, biosensors, tissue engineering, photodynamic and photothermal therapy, and drug delivery[10-12]. Magnetite nanoparticles have been used in water treatment to remove of heavy metals from water bodies[13], and they can be used effectively in photocatalytic processes[14]. Due to their characteristics, and the versatile and broad application fields, this study aimed to synthesize the magnetite and silica nanoparticles using the facile, low-coast, and time-saving preparation methods.

. II. Materials and Methods

2.1. Materials

For the silicon dioxide nanoparticles preparation, silica-gel 60/120 mesh [for cc] was purchased from ALFA CHEMIKA (India), and hydrochloric acid HCl from ADWIC (EL-Nasr pharmaceutical chemicals company, (Egypt). Ferric nitrate and ammonium ferrous sulfate were obtained from ALFA CHEMIKA (India) for the preparation of magnetite nanoparticles. Sodium hydroxide used during this wok was supplied by LOBAL CHEMIE (India).

2.2. Apparatus and procedure:

2.2.1. Silica nanoparticles preparation

Silica nanoparticles were synthesized via the sol-gel method, where 2.4 g of silica gel was dissolved in 0.08 mol of sodium hydroxide solution, thereafter, 0.1 g of   CETRIMIDE surfactant was added to the blend, and the mixture was magnetically stirred to obtain a homogeneous solution. An aqueous solution of hydrochloric acid (1M HCl) was dropwise added. A colorless gel-like precipitate was formed. Then the precipitate was washed with distilled water to remove the unwanted products, and dried in an oven at 80 ℃ overnight. The calcination of produced precipitate was performed in the muffle furnace at 800 ℃ for 4 h.

2.2.2. Magnetite nanoparticles preparation

Magnetite nanoparticles were prepared using the hydrothermal method. Two different iron salts, 9.9 mmol of ferric nitrate and 5 mmol ammonium ferrous sulfate were dissolved in 30 mL distilled water and added to a 5 mmol/mL NaOH solution. Thereafter, 0.1 g of surfactant CETRIMIDE was added. After magnetic stirring for 3 h at room temperature, a 100 ml Teflon-lined stainless-steel autoclave was charged with the reaction blend and placed in an oven at 100 ℃ for 1 h. The precipitate was isolated by decantation after allowing the autoclave to reach room temperature naturally and the precipitate was washed several times with distilled water and dried in an oven at 80℃ overnight.

2.2.3. Characterization apparatus of as-prepared nanoparticles

The structure of the as-prepared nanoparticles was characterized using the energy dispersive x-ray spectroscopy for the silica sample (EDS). X-ray diffraction (XRD), collected by an 18 kW diffractometer (Bruker; model D8 advance) with monochromator Cu-Ka radiation (1.54178 Å). Fourier transform infrared (FT-IR) spectra were obtained using a FT-IR spectrometer (Thermo Fisher-Nicolet IS10) from 4000 to 400 cm^{-1} at room temperature. The morphology of as-synthesized nanoparticles was characterized by Transmission electron microscopy (TEM) images were taken by electron microscope (JEM 2100) at an accelerating voltage of 200 kV; where the sample was dispersed in ethanol on a copper grid, and Scanning electron microscopy (SEM) images analysis was captured using a field emission electron microscope (FE-SEM) with a microscope (JEOL JSM-6500F).

III. RESULTS And DISCUSSION

3.1. The elemental analysis spectrum of silica nanoparticles (S)

The elemental analysis of as-synthesized silica nanoparticles (S) was investigated using the energy dispersive x-ray spectroscopy (EDS) technique figure (1). The EDS chart showed the peaks of oxygen (**O**), and silicon (**Si**) with weight percent of 43.12 and 47.41wt% respectively, and the existence of oxygen peak was indicated to the formation of SiO$_2$. The spectrum also showed a peak revealed to (**Au**) 4.13wt%, due to the gold covering film on the Cu grid of the apparatus used, and no other peaks of any impurities.
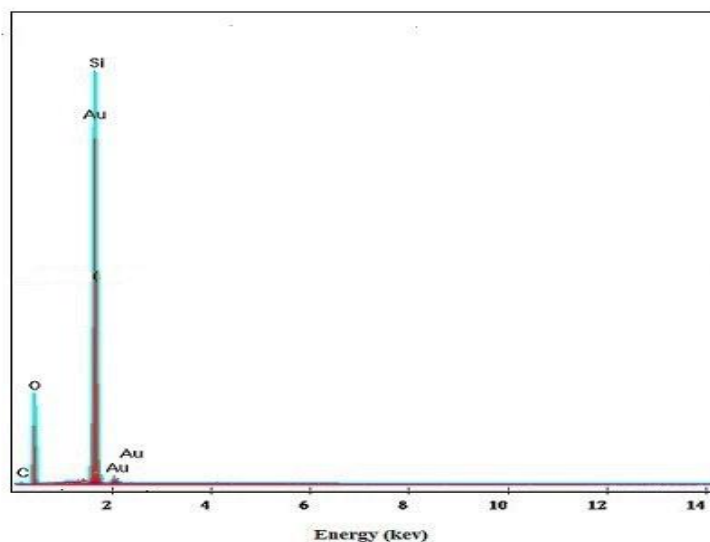
Fig. 1. The EDS spectra of as-prepared silica nanoparticles (S).

3.2. X-ray diffraction

The x-ray diffraction patterns of fabricated nanoparticles were depicted in fig. (2) showed XRD patterns with the characteristic peaks of magnetite (M) were observed at 2θ values of 30º,35º, 43º, 54º, 57ºand 62º, marked by (220), (311), (400), (422), (511), and (440) planes according to miller indices. The position and relative intensity of the peaks in the obtained XRD pattern matches well with the standard magnetite samples[15]. According to ICSD file No. 01-089-0688, this data demonstrates that this magnetite (M) sample is in an inverse spinel structure with a face-centered cubic phase with a calculated average crystallite size of 4nm using the Debye-Scherrer equation:

$$D = \frac{K\lambda}{\beta Cos\theta} \quad (1)$$

Where; D is the crystallite size (nm), k is a constant = 0.9, λ is the wavelength of radiation = 1.54060 Å (in the case of Cu Kα), β is the full width of half maximum in the radian, and θ is the diffraction angle in radian.

On the other hand, the XRD pattern of synthesized silica nanoparticles(S) figure 2 shows reflection peaks at 2θ values of 19.489º, 20.578º, 21.102º, 22.7º, 23.27º, where its planes are indexed according to miller indices (hkl), (111), (204), (112), (204), (006), which is inconsistent with the standard pattern of monoclinic silica phase tridymite (space group Cc, ICSD card 01-076-0894)[16]. And the reflection peaks at 2θ values 21.94º, 28.39º, 36º, 46.91º, 53.6º, 57.76º, 60.22º, and 64.96º with (hkl) planes index; (101), (111), (200), (113), (221), (301), (311), and (312) respectively attributed to the other phase of silica cristobalite, (space

group P41212, ICSD card 01-076-0935). The average crystallite size (D) of as-prepared silica nanoparticles was calculated using the above Debye-Scherrer equation (1) to be 37 nm.
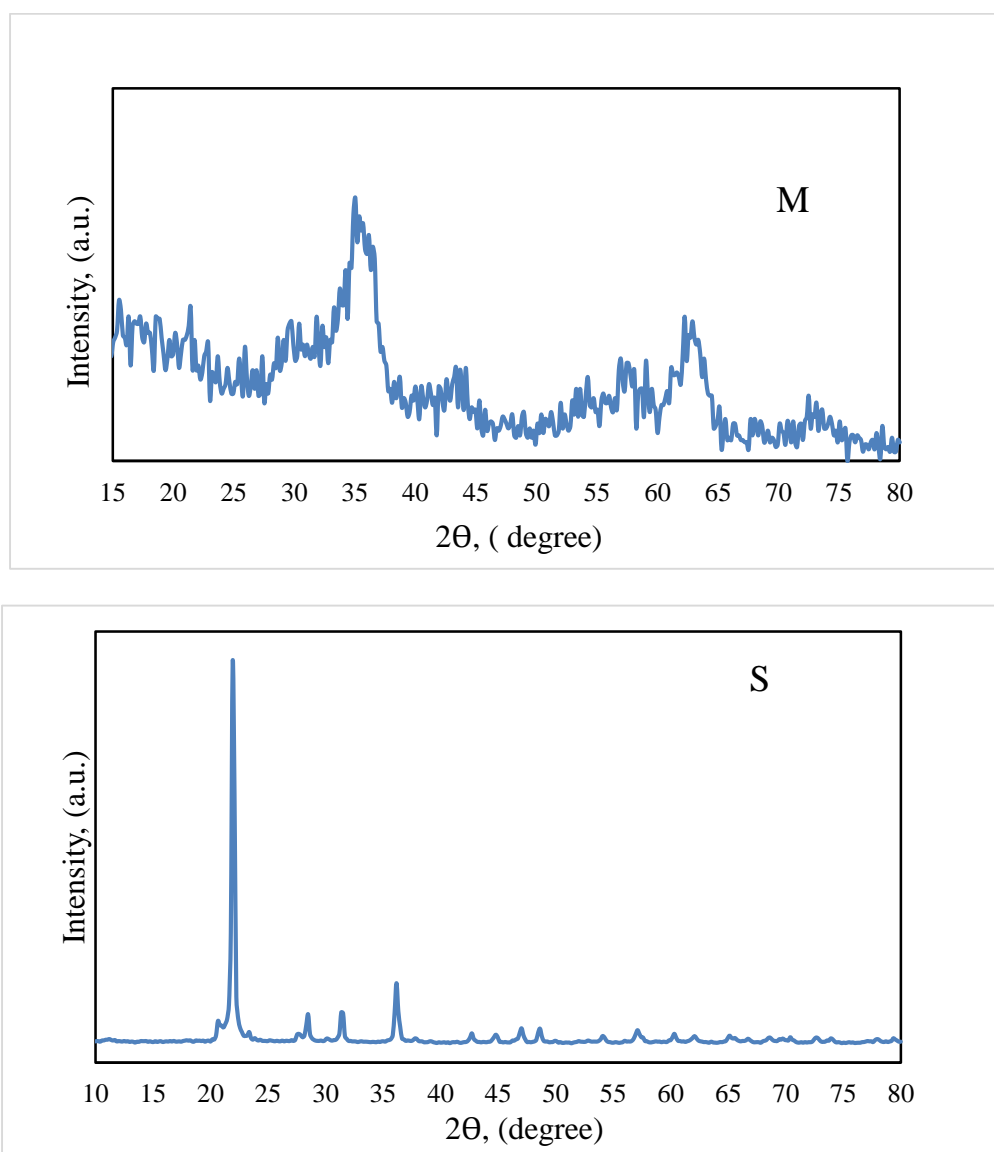

Fig. 2. XRD patterns of as-synthesized magnetite (M), and silica (S) nanoparticles

3.3. Fourier transforms infrared (FT-IR) study

The structure of as-prepared magnetite (M) was elucidated using the FT-IR spectrum. The IR spectra (figure 3 M) showed quite a similar magnetite (M) characterizing frequencies at around 434, 570, and 630 cm^{-1} which are characteristic of bare magnetite[17, 18]. The band near 570 cm^{-1} is related to stretching vibrations of the Fe-O functional group[19, 20]. The band around 630 cm^{-1} corresponds to the octahedral vibrational matrix[21]. The band near 1400 cm^{-1} can be attributed to O-H bond binding. The two bands at 1600 and 3370 cm^{-1} can be attributed to the stretching and bending vibrations of adsorbed surface water molecules interacting with the oxide product and the broadness of these peaks may be assigned to hydrogen bonding O–H[22, 23].

On the other hand, Infra-red analysis of fabricated silica nanoparticles (S) fig. 3, showed that the characteristic frequencies at 470 cm^{-1}, and 797 cm^{-1} are related to stretching vibrations of Si-O-Si[24], the band appeared at 1101cm^{-1} Si-O-Si asymmetric fluctuation[25, 26]. The absorption band at 2000 cm^{-1} corresponds to the silica matrix skeletal vibration[27].
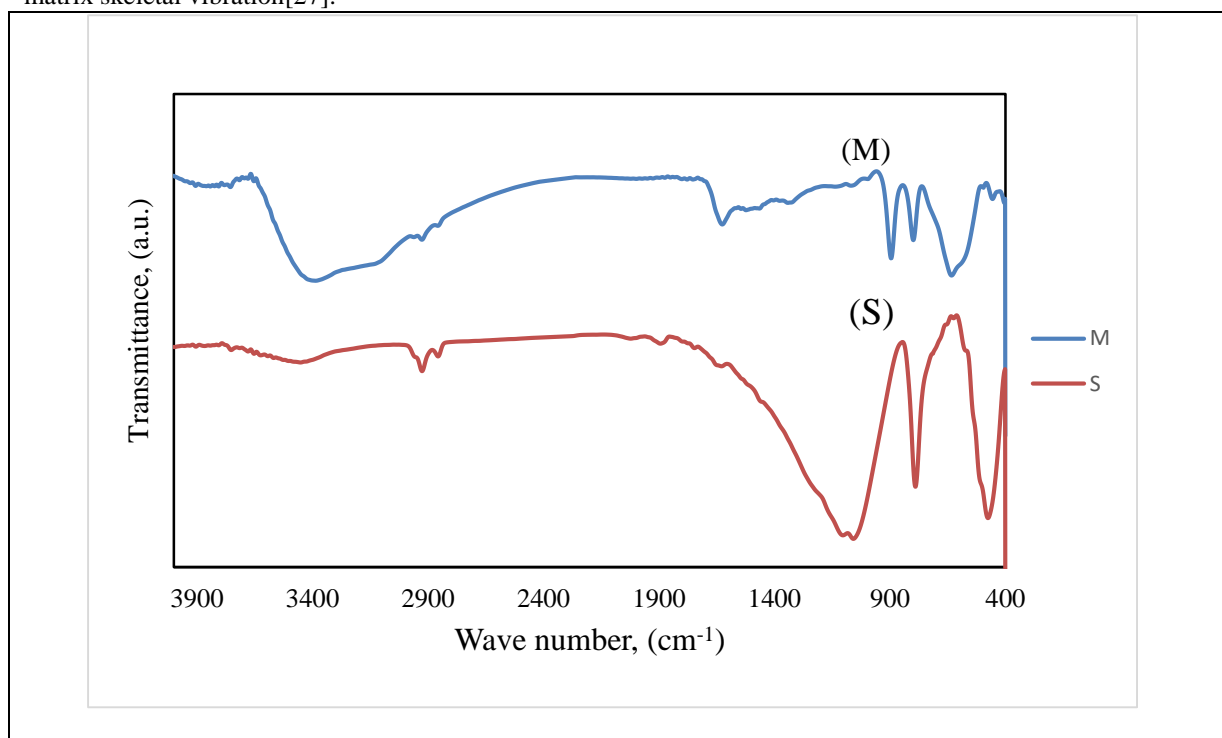
Fig. 3. FT-IR spectra of synthesized magnetite (M), and silica (S) nanoparticles.

3.4. Morphological studies

The morphology of the synthesized nanoparticles (M and S), was analyzed using the electronic microscope. Transmission electron microscope (TEM) images of fabricated magnetite (fig. 4 M) samples showed irregular morphology, uncompleted hexagonal shapes, and spherical particles with an estimated average particle size of 4nm which is in good agreement with the calculated size from XRD data. The TEM images also exhibited a little agglomeration of the particles due to the high magnetic character of magnetite nanoparticles. But TEM image of prepared silica (fig. 4 S) exhibits that the SiO$_2$ product consists of spherical and irregular morphology with an average particle size of ca. 15nm which is consistent with XRD results.
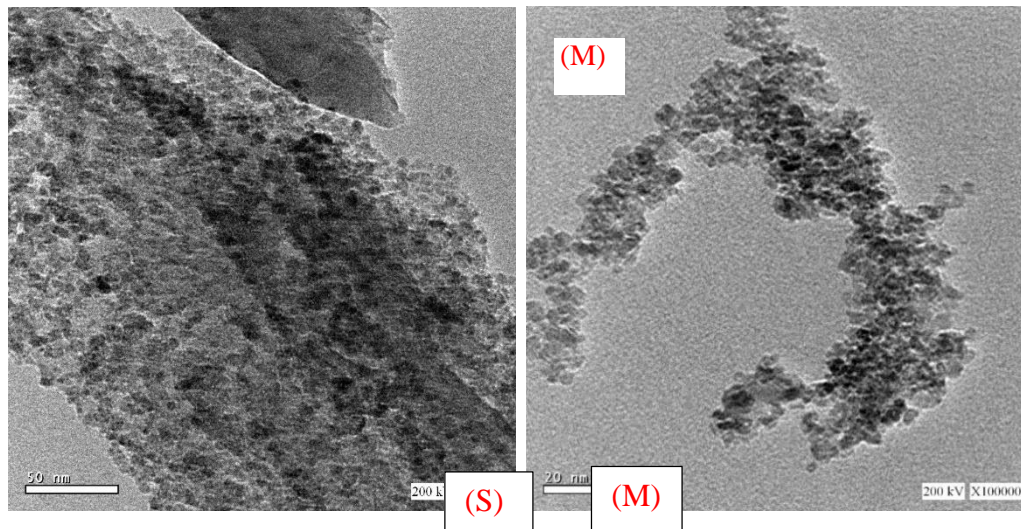
Fig. 4. HR-TEM images of fabricated magnetite (M), and silica (S) nanoparticles.

On the other hand, the scanning electron microscope (SEM) technique was employed to more confirmation of the morphology of fabricated nanoparticles. The (SEM) image of prepared magnetite nanoparticles (fig. 5 M) showed spherical, nonspherical, and nondispersed shapes and the grain size was determined to be in the range of 50 nm. The FE-SEM image of synthesized silica nanoparticles (fig. 5 S) showed spherical grains and peanut-shaped particles, and the grain size was determined to be in the range of 0.5µm.
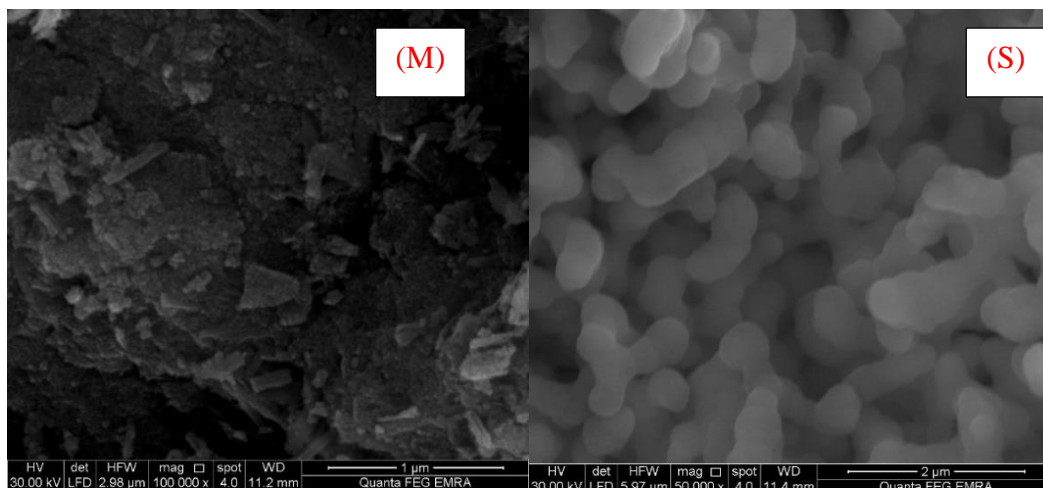
Fig. 5. SEM images of fabricated magnetite (M), and silica (S) nanoparticles.

IV.Discussion

In this study, we have prepared magnetite and silicon dioxide nanoparticles using a simple and facile synthesis method, hydrothermal and sol-gel respectively. The prepared nanoparticles were studied and characterized by EDS, XRD, FT-IR, HR-TEM, and FE-SEM techniques. The obtained data showed that the crystal sizes of magnetite and silica were 4 nm, and 37 nm respectively, with defined morphologies of as-prepared (M) and (S) with the grain sizes of 50 nm, and .05 µm respectively.

REFERENCES

1. **Biswas, P. and C.-Y. Wu, *Nanoparticles and the environment.* Journal of the air & waste management association, 2005. 55(6): p. 708-746.**

2. Banfield, J.F. and H. Zhang, *Nanoparticles in the environment.* Reviews in mineralogy and geochemistry, 2001. **44**(1): p. 1-58.

3. Petros, R.A. and J.M. DeSimone, *Strategies in the design of nanoparticles for therapeutic applications.* Nature reviews Drug discovery, 2010. **9**(8): p. 615-627.

4. Cao, G., *Nanostructures and Nanomaterials: Synthesis, Properties and Applications*. 2004, World Scientific.

5. Moreno-Vega, A.-I., et al., *Polymeric and Ceramic Nanoparticles in Biomedical Applications.* Journal of Nanotechnology, 2012. **2012**: p. 936041.

6. C Thomas, S., P. Kumar Mishra, and S. Talegaonkar, *Ceramic nanoparticles: fabrication methods and applications in drug delivery.* Current pharmaceutical design, 2015. **21**(42): p. 6165-6188.

7. Singh, D., et al., *Ceramic nanoparticles: Recompense, cellular uptake and toxicity concerns.* Artificial Cells, Nanomedicine, and Biotechnology, 2016. **44**(1): p. 401-409.

8. Kumar, R., et al., *Advances in nanotechnology and nanomaterials based strategies for neural tissue engineering.* Journal of Drug Delivery Science and Technology, 2020. **57**: p. 101617.

9. Gawande, M.B., P.S. Branco, and R.S. Varma, *Nano-magnetite (Fe3O4) as a support for recyclable catalysts in the development of sustainable methodologies.* Chemical Society Reviews, 2013. **42**(8): p. 3371-3393.

10. Kemp, S.J., et al., *Monodisperse magnetite nanoparticles with nearly ideal saturation magnetization.* RSC Advances, 2016. **6**(81): p. 77452-77464.

11. Mirabello, G., J.J.M. Lenders, and N.A.J.M. Sommerdijk, *Bioinspired synthesis of magnetite nanoparticles.* Chemical Society Reviews, 2016. **45**(18): p. 5085-5106.

12. Gnanaprakash, G., et al., *Effect of initial pH and temperature of iron salt solutions on formation of magnetite nanoparticles.* Materials Chemistry and Physics, 2007. **103**(1): p. 168-175.

13. Anastasova, E.I., et al., *A pure magnetite hydrogel: synthesis, properties and possible applications.* Soft Matter, 2017. **13**(45): p. 8651-8660.

14. Alfredo Reyes Villegas, V., et al., *Synthesis and characterization of magnetite nanoparticles for photocatalysis of nitrobenzene.* Journal of Saudi Chemical Society, 2020. **24**(2): p. 223-235.

15. Fjellvåg, H., et al., *On the crystallographic and magnetic structures of nearly stoichiometric iron monoxide.* Journal of Solid State Chemistry, 1996. **124**(1): p. 52-57.

16. Dollase, W. and W. Baur, *The superstructure of meteoritic low tridymite solved by computer simulation.* American Mineralogist, 1976. **61**(9-10): p. 971-978.

17. Abdel-Bary, A.S., et al., *Chitosan, magnetite, silicon dioxide, and graphene oxide nanocomposites: Synthesis, characterization, efficiency as cisplatin drug delivery, and DFT calculations.* International Journal of Biological Macromolecules, 2020. **154**: p. 621-633.

18. Ramadan, I. and M. Moustafa, *Egyptian Journal of.* 2022.

19. Nassar, M.Y. and M. Khatab, *Cobalt ferrite nanoparticles via a template-free hydrothermal route as an efficient nano-adsorbent for potential textile dye removal.* RSC advances, 2016. **6**(83): p. 79688-79705.

20. Nassar, M.Y., et al., *A controlled, template-free, and hydrothermal synthesis route to sphere-like α-Fe 2 O 3 nanostructures for textile dye removal.* Rsc Advances, 2016. **6**(24): p. 20001-20013.

21. Cornell, R.M. and U. Schwertmann, *The iron oxides: structure, properties, reactions, occurrences, and uses*. Vol. 2. 2003: Wiley-vch Weinheim.

22. Nassar, M.Y., M.M. Moustafa, and M.M. Taha, *Hydrothermal tuning of the morphology and particle size of hydrozincite nanoparticles using different counterions to produce nanosized ZnO as an efficient adsorbent for textile dye removal.* RSC advances, 2016. **6**(48): p. 42180-42195.

23. Nassar, M.Y. and S. Abdallah, *Facile controllable hydrothermal route for a porous CoMn 2 O 4 nanostructure: synthesis, characterization, and textile dye removal from aqueous media.* RSC advances, 2016. **6**(87): p. 84050-84067.

24. Nassar, M.Y., I.S. Ahmed, and M.A. Raya, *A facile and tunable approach for synthesis of pure silica nanostructures from rice husk for the removal of ciprofloxacin drug from polluted aqueous solutions.* Journal of Molecular Liquids, 2019. **282**: p. 251-263.

25. El-Feky, H.H., et al., *Facile Fabrication of Nano-sized SiO2 by an Improved Sol–Gel Route: As an Adsorbent for Enhanced Removal of Cd (II) and Pb (II) Ions.* Journal of Inorganic and Organometallic Polymers and Materials, 2022. **32**(3): p. 1129-1141.

26. Baz, M.M., et al., *Efficacy of porous silica nanostructure as an insecticide against filarial vector Culex pipiens (Diptera: Culicidae).* International Journal of Tropical Insect Science, 2022: p. 1-13.

27. Sonin, D.L., et al., *Silicon-containing nanocarriers for targeted drug delivery: Synthesis, physicochemical properties and acute toxicity.* Drug delivery, 2016. **23**(5): p. 1747-1756.